

# Charged $\rho$ meson production in neutrino-induced reactions at $\langle E_\nu \rangle \approx 10$ GeV

SKAT Collaboration

N.M. Agababyan<sup>1</sup>, V.V. Ammosov<sup>2</sup>, M. Atayan<sup>3</sup>,  
N. Grigoryan<sup>3</sup>, H. Gulkanyan<sup>3</sup>, A.A. Ivanilov<sup>2</sup>,  
Zh. Karamyan<sup>3</sup>, V.A. Korotkov<sup>2</sup>

<sup>1</sup> Joint Institute for Nuclear Research, Dubna, Russia

<sup>2</sup> Institute for High Energy Physics, Protvino, Russia

<sup>3</sup> Yerevan Physics Institute, Armenia

YEREVAN 2008

## Abstract

The neutrino production of charged  $\rho$  mesons on nuclei and nucleons is investigated for the first time at moderate energies ( $\langle E_\nu \rangle \approx 10$  GeV), using the data obtained with SKAT bubble chamber. No strong nuclear effects are observed in  $\rho^+$  and  $\rho^-$  production. The fractions of charged and neutral pions originating from  $\rho$  decays are obtained and compared with higher energy data. From analysis of the obtained and available data on  $\rho^+$  and  $K^{*+}(892)$  neutrino production, the strangeness suppression factor in the quark string fragmentation is extracted:  $\lambda_s = 0.18 \pm 0.03$ . Estimations are obtained for cross sections of quasiexclusive single  $\rho^+$  and coherent  $\rho^+$  neutrino production on nuclei. The estimated coherent cross section  $\sigma_{\rho^+}^{coh} = (0.29 \pm 0.16) \cdot 10^{-38}$  cm<sup>2</sup> is compatible with theoretical predictions.

# 1 Introduction

In order to infer as comprehensive as possible information about the space-time pattern of leptoproducted quark string fragmentation processes, experimental data on nuclear targets are needed, not only concerning the production of stable hadrons, but also hadronic resonances. At present, more or less detailed experimental data collected in neutrino-nuclear interactions are available only for neutral  $\rho$  mesons ([1, 2, 3] and references therein), while those for charged  $\rho$  mesons are rather scarce and obtained at comparatively high energies of (anti)neutrino,  $\langle E_\nu \rangle \sim 40\text{-}50$  GeV [2]. The aim of this work is to study the neutrino-production of  $\rho^+$  and  $\rho^-$  mesons in neutrino-nucleus ( $\nu$  A) and neutrino-nucleon ( $\nu$  N) charged current interactions at intermediate energies ( $\langle E_\nu \rangle \sim 10$  GeV). In Section 2, the experimental procedure is described. Section 3 presents the experimental data including: a) the inclusive production of  $\pi^0$  mesons; b) the mean multiplicities of  $\rho^+$  and  $\rho^-$  mesons and the ratios of  $\rho$  meson to pion yields, compared to the data at higher energies [2]; c) the quasiexclusive and coherent single  $\rho^+$  neutrino-production on nuclear targets. The results are summarized in Section 4.

## 2 Experimental procedure

The experiment was performed with SKAT bubble chamber [4], exposed to a wideband neutrino beam obtained with a 70 GeV primary protons from the Serpukhov accelerator. The chamber was filled with a propane-freon mixture containing 87 vol% propane ( $C_3H_8$ ) and 13 vol% freon ( $CF_3Br$ ) with the percentage of nuclei H:C:F:Br = 67.9:26.8:4.0:1.3 %. A 20 kG uniform magnetic field was provided within the operating chamber volume.

Charged (CC) current interactions containing a negative muon with momentum  $p_\mu > 0.5$  GeV/c were selected. Other negatively charged particles were considered to be  $\pi^-$  mesons. Protons with momentum below 0.6 GeV/c and a fraction of protons with momentum 0.6-0.85 GeV/c were identified by their stopping in the chamber. Non-identified positively charged particles were considered to be  $\pi^+$  mesons. Events in which errors in measuring the momenta of all charged secondaries and photons were less than 60% and 100%, respectively, were selected. The mean relative error  $\langle \Delta p/p \rangle$  in the momentum measurement for muons, pions and gammas was, respectively, 3%, 6.5% and 19%. Each event is given a weight which corrects for the fraction of events excluded due to improperly reconstruction. More details concerning the experimental procedure, in particular, the reconstruction of the neutrino energy  $E_\nu$  can be found in our previous publications [5, 6].

The events with  $3 < E_\nu < 30$  GeV were accepted, provided that the reconstructed mass  $W$  of the hadronic system exceeds 1.8 GeV. No restriction was imposed on the transfer momentum squared  $Q^2$ . The number of accepted events was 5011 (6868 weighted events). The mean values of the kinematical variables were  $\langle E_\nu \rangle = 9.8$  GeV,  $\langle W \rangle = 2.8$  GeV,  $\langle W^2 \rangle = 8.7$  GeV<sup>2</sup>,  $\langle Q^2 \rangle = 2.6$  (GeV/c)<sup>2</sup>.

Further, the whole event sample was subdivided, using several topological and kinematical criteria [6, 7], into three subsamples: the 'cascade' subsample  $B_S$  with a sign of intranuclear secondary interaction, the 'quasiproton' ( $B_p$ ) and 'quasineutron' ( $B_n$ ) subsamples. About 40% of subsample  $B_p$  is contributed by interactions with free hydrogen. Weighting the 'quasiproton' events with a factor of 0.6, one can compose a 'pure' nuclear subsample  $B_A = B_S + B_n + 0.6B_p$  and a 'quasinucleon' subsample  $B_N = B_n + 0.6B_p$ . It has been verified

[7, 8], that the multiplicity and spectral characteristics of secondary particles in the  $B_p(B_N)$  subsample are in satisfactory agreement with those measured with a pure proton (deuteron) target. The effective atomic weight corresponding to the subsample  $B_A$  is estimated [6] to be approximately equal to  $A_{eff} = 21 \pm 2$ , when taking into account the probability of secondary intranuclear interactions in the composite target.

### 3 Results

a) The inclusive production of  $\pi^0$  meson

The proper reconstruction of  $\pi^0 \rightarrow 2\gamma$  decays is the main prerequisite for that of  $\rho^\pm \rightarrow \pi^0\pi^\pm$  decays. Fig. 1 shows the two-gamma effective mass distribution for the total sample of events corrected for losses of non-registered or rejected  $\gamma$ -quanta (see [10] for details). The  $m_{\gamma\gamma}$  - distribution was fitted as a sum of non-relativistic Breit-Wigner function, with the pole mass  $m_0$  and width  $\Gamma_0$  as free parameters, and the background distribution of the form

$$BG_0 \sim m_{\gamma\gamma}^\alpha \exp(\beta m_{\gamma\gamma} + \gamma m_{\gamma\gamma}^2) , \quad (1)$$

with  $\alpha$ ,  $\beta$  and  $\gamma$  as free parameters. The fitted values of  $m_0 = 0.139 \pm 0.002$  GeV/ $c^2$  and  $\Gamma_0 = 0.055 \pm 0.007$  GeV turn out to be compatible with the  $\pi^0$  mass and experimental resolution (estimated from Monte-Carlo simulation), respectively. A similar fitting procedure, but with fixed  $m_0 = 0.135$  GeV/ $c^2$  and  $\Gamma_0 = 0.055$  GeV, was applied for the quasinucleon and nuclear subsamples, resulting in the  $\pi^0$  mean multiplicities  $\langle n_{\pi^0} \rangle_N = 0.787 \pm 0.080$  and  $\langle n_{\pi^0} \rangle_A = 0.904 \pm 0.066$ , respectively. The nuclear enhancement factor for the  $\pi^0$  yield,  $R_{\pi^0} = \langle n_{\pi^0} \rangle_A / \langle n_{\pi^0} \rangle_N = 1.15 \pm 0.14$ , practically coincides with that for  $\pi^-$  meson,  $R_{\pi^-} = 1.12 \pm 0.03$  (see also [3, 8, 9]), quantitatively explained by secondary intranuclear interaction processes [8, 9].

In the next subsection, where the effective mass distributions of  $\pi^+\gamma\gamma$  and  $\pi^-\gamma\gamma$  systems are analyzed, only two-gamma combinations with  $0.105 < m_{\gamma\gamma} < 0.165$  GeV/ $c^2$  will be kept.

b) Mean multiplicities of charged  $\rho$  mesons

Fig. 2 shows the effective mass distributions for  $\pi^+\gamma\gamma$  and  $\pi^-\gamma\gamma$  systems, both for nuclear and quasinucleon subsamples, corrected for losses of reconstructed  $\pi^0$  and contamination from the background  $\gamma\gamma$  combinations. A clear signal for  $\rho^+$ , but a faint one for  $\rho^-$  are seen. The distribution were fitted by the form

$$dN/dm = BG \cdot (1 + \alpha_\rho BW_\rho) , \quad (2)$$

where the mass dependence of the background was parametrized as

$$BG = \alpha_1 \exp(\alpha_2 m + \alpha_3 m^2) , \quad (3)$$

with  $m \equiv m_{\pi^+\gamma\gamma}$  or  $m_{\pi^-\gamma\gamma}$  and  $\alpha_1$ ,  $\alpha_2$ ,  $\alpha_3$  being free parameters, while for  $BW_\rho$  the relativistic Breit-Wigner function [11] was used, with fixed pole mass  $m_\rho = 0.776$  GeV/ $c^2$  and width  $\Gamma_\rho = 0.149$  GeV [12]. The experimental mass resolution was taken into account by replacing  $\Gamma_\rho$  by  $\sqrt{\Gamma_\rho^2 + \Gamma_{res}^2}$  with  $\Gamma_{res} = 0.11$  GeV estimated from Monte-Carlo simulations. A similar analysis was also performed for the  $\pi^+\gamma\gamma$  system produced in the forward ( $x_F > 0$ ,  $x_F$  being the Feynman variable) and backward ( $x_F < 0$ ) hemispheres in the hadronic

c.m.s.

The resulting mean yields of charged  $\rho$  mesons are presented in Table 1. It should be emphasized, that the sum of extracted yield of  $\rho^+$  at  $x_F < 0$  and  $x_F > 0$  is in good agreement with the total yield. As expected, the yield of unfavorable  $\rho^-$  (not containing the current quark) is much smaller than that of favorable  $\rho^+$  (which can contain the current quark). The data do not reveal, due to comparatively large statistical errors, significant nuclear effects in charged  $\rho$  neutrino production, perhaps except a faint indication on the shifting the  $\rho^+$   $x_F$  - distribution in the nuclear interactions towards backward hemisphere as compared to quasinucleon interactions. A similar effect, but better expressed, was observed recently for  $\rho^0$  mesons, indicating on a non-negligible role of secondary intranuclear interaction processes [3].

Table 1: The mean multiplicities of  $\rho^+$  and  $\rho^-$  mesons in quasinucleon and nuclear interactions.

A	$\langle n_{\rho^+} \rangle$			$\langle n_{\rho^-} \rangle$
	all $x_F$	$x_F < 0$	$x_F > 0$	all $x_F$
1	$0.101 \pm 0.032$	$0.046 \pm 0.033$	$0.061 \pm 0.030$	$0.026 \pm 0.024$
21	$0.120 \pm 0.031$	$0.067 \pm 0.025$	$0.051 \pm 0.015$	$0.039 \pm 0.015$

c) The  $W$ - dependence of the  $\rho$  yield and the ratio of  $\rho$  and pion yields

Fig. 3 shows the  $W$  - dependence of the charged  $\rho$  yields measured in this work for  $\nu A$  - interactions at  $W = 2.8$  GeV and in [2] for  $\nu(\bar{\nu})Ne$  - interactions. For comparison, the data for favorable vector mesons  $\rho^0$  [2, 3] and  $K^{*+}(892)$  ([13] and references therein) are also plotted. The  $W$  - dependence of the mean yields can be approximately described by a simplest linear form  $b \cdot (W - W_0)$  at the fixed threshold value  $W_0 = 1.8$  GeV. The fitted slope parameters  $b$  are given in Table 2.

Table 2: The slope parameter  $b$  (in  $\text{GeV}^{-1}$ ).

Reaction	all $x_F$	$x_F < 0$	$x_F > 0$
$\nu \rightarrow \rho^+$ or $\bar{\nu} \rightarrow \rho^-$	$0.091 \pm 0.011$	$0.037 \pm 0.007$	$0.046 \pm 0.006$
$\nu \rightarrow \rho^0$ or $\bar{\nu} \rightarrow \rho^0$	$0.056 \pm 0.007$	$0.014 \pm 0.005$	$0.045 \pm 0.004$
$\nu \rightarrow \rho^-$ or $\bar{\nu} \rightarrow \rho^+$	$0.021 \pm 0.007$		
$\nu \rightarrow K^{*+}(892)$	$0.017 \pm 0.002$		

As it is seen from Table 2 and Fig. 3, the yields of favorable charged and neutral  $\rho$ 's are the same in the forward hemisphere, testifying that the current quark  $u$  (or  $\bar{d}$ ) recombines with sea antiquarks (quarks)  $\bar{u}$  and  $\bar{d}$  (or  $d$  and  $u$ ) with equal probabilities. On the other hand, the yield of the favorable charged  $\rho$  exceeds that of  $\rho^0$  in the backward hemisphere.

The ratio  $b(K^{*+})/b(\rho^+)$  can serve as an almost direct estimation for the strange quark suppression factor  $\lambda_s \equiv (\bar{s}/\bar{u})$  during the string fragmentation at the considered  $W$ - range:  $\lambda_s = 0.18 \pm 0.03$ . This value is compatible with estimations extracted from hadronic interactions ([14, 15] and references therein).

Fig. 4 presents the  $\langle n_{\rho} \rangle_A / \langle n_{\pi} \rangle_A$  ratios extracted from [2] and obtained in this work, using the

measured pion yields  $\langle n_{\pi^0} \rangle_A = 0.904 \pm 0.066$ ,  $\langle n_{\pi^-} \rangle_A = 0.652 \pm 0.010$  and  $\langle n_{\pi^+} \rangle_A = 1.55 \pm 0.06$  (the latter error being caused mainly by the uncertainty in the extraction of the contamination from non-identified protons). As it is seen from the left panel of Fig. 4, the fraction of  $\pi^0$  originating from decays of favorable and unfavorable  $\rho$ 's is practically independent of  $\langle W \rangle$  (in the considered range  $2.8 < \langle W \rangle < 4.8$  GeV) and composes on an average  $14.2 \pm 1.8$  and  $3.4 \pm 1.0\%$ , respectively (indicated by dashed lines in Fig. 4). The latter value is close to the fraction of charged pions from the decay of unfavorable  $\rho$ , composing on an average  $4.3 \pm 1.3\%$  (open symbols and the dashed line in the right panel of Fig. 4). Unlike the latter and neutral pions, the fraction of charged pions originating from the favorable  $\rho$  decay tends to increase with  $\langle W \rangle$ , varying from  $7.7 \pm 2.0\%$  at  $\langle W \rangle = 2.8$  GeV to  $12.6 \pm 2.9\%$  at  $\langle W \rangle = 4.8$  GeV (closed symbols in the right panel of Fig. 4).

d) Quasiexclusive and coherent single  $\rho^+$  production on nuclei

This subsection is devoted to the estimation of cross sections of quasiexclusive and coherent single  $\rho^+$  production in the reaction

$$\nu A \rightarrow \mu^- + (\pi^+ \gamma \gamma) + X_0, \quad (4)$$

where the state  $X_0$  does not contain any visible tracks.

The rate of the quasiexclusive reaction

$$\nu A \rightarrow \mu^- + (\pi^+ \pi^0) + X_0 \quad (5)$$

extracted from the  $m_{\gamma\gamma}$  - distribution, plotted in Fig. 5a, is equal to  $R(\nu A \rightarrow \mu^- \pi^+ \pi^0 X_0) = (2.4 \pm 0.4) \cdot 10^{-2}$ . The contamination to the latter from reactions where one or more additional (not registered)  $\pi^0$ 's are produced was estimated from the analysis of events containing more than two detected gammas. This contamination to the reaction (5) turns out to be rather small,  $(11 \pm 10)\%$ . As it is seen from Fig. 5a, the  $\pi^0$  mass region is practically free of background. This observation allows one to apply less severe cut on the 'usefull' range of  $m_{\gamma\gamma}$ ,  $0.053 < m_{\gamma\gamma} < 0.217$  GeV/ $c^2$ , thus reducing the  $\pi^0$  losses in the  $\pi^+ \gamma \gamma$  effective mass distribution.

The rate  $R(\mu^- \rho^+ X_0) = \sigma(\nu A \rightarrow \mu^- \rho^+ X_0) / \sigma(\nu A \rightarrow \mu^- X)$  of the quasiexclusive incoherent reaction

$$\nu A \rightarrow \mu^- \rho^+ X_0 \quad (6)$$

was estimated from the  $\pi^+ \gamma \gamma$  effective mass distribution (Fig. 5b) from which the events-candidates to the  $\rho^+$  coherent production (see below) were excluded. This distribution was corrected and fitted as described above in Subsection 3b resulting in  $R(\mu^- \rho^+ X_0) = (1.0 \pm 0.5) \cdot 10^{-2}$ . The latter composes only  $(8.5 \pm 4.3)\%$  of the  $\rho^+$  production total rate (cf. Table 1) and corresponds to the cross section  $\sigma(\nu A \rightarrow \mu^- \rho^+ X_0) = (2.2 \pm 1.2) \cdot 10^{-38}$  cm<sup>2</sup> obtained at calculated  $\nu A$  cross section  $\sigma(\nu A \rightarrow \mu^- X) = (1.16 \pm 0.09) \cdot 10^{-36}$  cm<sup>2</sup> at  $\langle E_\nu \rangle = 9.8$  GeV, using the known neutrino-nucleon CC cross sections  $\sigma_{\nu p}^{CC} / E_\nu = (0.50 \pm 0.04) \cdot 10^{-38}$  cm<sup>2</sup>/GeV and  $\sigma_{\nu n}^{CC} = 2\sigma_{\nu p}^{CC}$  ([12, 16] and references therein) and taking into account the nuclei content of the composite target.

As the process (6) occurs on intranuclear neutrons, the number of events belonging to that reaction can be normalized to the number of events of quasineutron subsample (see Section 3), leading to an estimation of the rate  $R(\mu^- \rho^+ n) = \sigma(\nu n \rightarrow \mu^- \rho^+ n) / \sigma(\nu n \rightarrow \mu^- X) = (4.4 \pm 2.2) \cdot 10^{-2}$ . Note, that this value (estimated for the first time for  $\nu n$ - interactions) turns out to be significantly larger than for reaction  $\nu p \rightarrow \mu^- \rho^+ p$  on free protons, measured

at a higher energy range ( $\langle E_\nu \rangle = 15$  GeV),  $R(\mu^+\rho^+p) = (0.7 \pm 0.2) \cdot 10^{-2}$  [17].

A particular case of quasiexclusive reaction (4) is the exclusive reaction of coherent  $\rho^+$  neutrino production

$$\nu A \rightarrow \mu^- \rho^+ A, \quad (7)$$

where the final nucleus remains in its ground state. This process is characterized by very small values of the squared four-momentum transfer  $|t| < t_{max} \approx 1/R_A^2$  to the nucleus of radius  $R_A$ . Even for the case of the lightest target nucleus ( $^{12}\text{C}$ ),  $t_{max} = 0.006$  (GeV/c) $^2$  being much smaller than the experimental resolution estimated from Monte-Carlo simulations,  $\sigma(t) \approx 0.06$  (GeV/c) $^2$ .

The squared four-momentum transfer  $|t|$  was estimated as

$$|t| = \left[ \sum_i (E_i - p_i^L) \right]^2 + \left( \sum_i \mathbf{p}_i^t \right)^2, \quad (8)$$

where  $E_i$ ,  $p_i^L$  and  $\mathbf{p}_i^t$  are, respectively, the energy, longitudinal and transverse momenta of detected final particles in the reaction (4). The  $|t|$  - distribution is shown in Fig. 5c, together with that for background (incoherent) events of reaction (4) containing observable products of the target nucleus desintegration not taken into account in evaluation of  $|t|$ . The background distribution is normalized to the former one at  $|t| > 0.09$  (GeV/c) $^2$ . As it is seen, coherent-like and incoherent events are distributed similarly at  $|t| > 0.09$  (GeV/c) $^2$ , while in the 'coherence' region  $|t| < 0.09$  (GeV/c) $^2$  there is a clear excess of coherent-like events (8 events) over incoherent one (one event). It has been also verified, via analysis of events with more than two detected  $\gamma$ 's, that the sample of coherent-like events is not contaminated by processes of two or more  $\pi^0$  production.

For all selected 8 events, the effective mass  $m_{\pi+\gamma\gamma}$  turns out to be enclosed in the region near the  $\rho$  pole mass,  $0.48 \leq m_{\pi+\gamma\gamma} \leq 1.08$  GeV/c $^2$ , with the mean value  $\langle m_{\pi+\gamma\gamma} \rangle = 0.7$  GeV/c $^2$  (Fig. 5d). This allows to assume, that the most part of these events originate from coherent reaction. The upper (lower) limit of the rate  $R_{\rho^+}^{coh}$  can be estimated assuming that all 8 events (6 events with  $0.58 \leq m_{\pi+\gamma\gamma} \leq 1.08$  GeV/c $^2$ ) correspond to coherent  $\rho^+$  production. Excluding the contamination from one incoherent event, as well as introducing a correction for losses due to the cut  $|t| < t_{max}$  (composing 8%), one obtains for upper and lower limits:  $R_{\rho^+}^{coh}(up) = (0.28 \pm 0.12) \cdot 10^{-2}$ , and  $R_{\rho^+}^{coh}(low) = (0.20 \pm 0.11) \cdot 10^{-2}$ . Note, that the average value of these estimations,  $R_{\rho^+}^{coh}(mean) = (0.24 \pm 0.12) \cdot 10^{-2}$  coincides practically with the value  $R_{\rho^+}^{coh}(fit) = (0.26 \pm 0.14) \cdot 10^{-2}$  extracted from the fit of data plotted in Fig. 5d by the relativistic Breit-Wigner distribution, taking also into account the contamination from one background event and the losses at  $|t| > t_{max}$ . As the final estimation for  $R_{\rho^+}^{coh}$ , we take the medial value  $R_{\rho^+}^{coh} = (0.25 \pm 0.14) \cdot 10^{-2}$ . Note, that the latter composes, respectively, (2.1 $\pm$ 1.3)% and (4.9 $\pm$ 3.1)% of the total and forward  $\rho^+$  production rates (cf. Table 1).

The estimated rate  $R_{\rho^+}^{coh} = (0.25 \pm 0.14) \cdot 10^{-2}$  can be compared with that obtained at higher-energy  $\nu Ne$  interactions [16],  $R_{\rho^+}^{coh}(10 < E_\nu < 320 \text{ GeV}) = (0.28 \pm 0.10) \cdot 10^{-2}$ . The quoted values do not contradict the expected slow variation of this rate ( $0.15 \cdot 10^{-2} < R_{\rho^+}^{coh} < 0.31 \cdot 10^{-2}$ ) in the wide range of  $10 < E_\nu < 300$  GeV, predicted on the basis of the vector dominance model (suggesting  $\rho$  meson dominance in the weak vector current) and Glauber theory ([18] and references therein).

The coherent  $\rho^+$  production cross section per target nucleus is equal to  $\sigma_{\rho^+}^{coh} = (0.29 \pm 0.16) \cdot 10^{-38}$  cm $^2$ . This value, plotted in Fig. 6 together with available data at higher  $E_\nu$  [19, 20], is compatible with the results of theoretical calculations [19] done in the framework of the  $\rho$  - dominance model for the case of  $Ne$  nucleus (the curve in Fig. 6).

## 4 Summary

The charged  $\rho$  meson neutrino production on nuclei and nucleons is investigated for the first time at moderate energies ( $\langle E_\nu \rangle \approx 10$  GeV). No strong nuclear effects are observed in  $\rho^+$  and  $\rho^-$  production.

The fractions of  $\pi^0$  mesons originating from the decay of favorable ( $\rho^+$ ) and that of  $\pi^0$  and  $\pi^-$  mesons from the decay of unfavorable ( $\rho^-$ )  $\rho$  mesons are found to be, respectively,  $13.3 \pm 3.6$ ,  $4.3 \pm 1.7$  and  $5.9 \pm 2.3\%$ , quite compatible with those obtained at higher energies, while this fraction for charged pions from favorable charged  $\rho$  tends to increase with  $W$ , varying from  $7.7 \pm 2.0\%$  at  $\langle W \rangle = 2.8$  GeV (this work) to  $12.6 \pm 2.9\%$  at  $\langle W \rangle = 4.8$  GeV [2].

From the obtained and available data on  $\nu(\bar{\nu})A \rightarrow \rho X$  reactions at  $\langle W \rangle = 2.8-4.8$  GeV, an indication is obtained that the yields of charged and neutral favorable  $\rho$  mesons in the forward hemisphere are practically the same, thus verifying that the struck current quark (antiquark) recombines with up and down sea antiquarks (quarks) with equal probabilities.

From analysis of the available data on  $\rho^+$  and  $K^{*+}(892)$  neutrino production at  $\langle W \rangle = 2.8-5.5$  GeV, an estimation is extracted for the strangeness suppression factor in the quark string fragmentation process:  $\lambda_s = 0.18 \pm 0.03$ .

For the first time, the rate of the single  $\rho^+$  production reaction on the neutron is estimated,  $R(\mu^- \rho^+ n) = (4.4 \pm 2.2) \cdot 10^{-2}$ .

An estimation is inferred for the cross section (per nucleus of the composite target) of the coherent  $\rho^+$  neutrino production on nuclei,  $\sigma_{\rho^+}^{coh} = (0.29 \pm 0.16) \cdot 10^{-38}$  cm<sup>2</sup>. The estimated coherent cross section is compatible with theoretical predictions based on the vector dominance model and the Glauber theory.

**Acknowledgement.** The activity of one of the authors (H.G.) is supported by Cooperation Agreement between DESY and YerPhI signed on December 6, 2002. The authors from YerPhI acknowledge the supporting grants of Calouste Gulbenkian Foundation and Swiss Fonds "Kidagan".

## References

- [1] V.V.Ammosov et al. (SKAT Coll.), *Yad. Fiz.* **46**, 131 (1987). [*Sov. J. Nucl. Phys.* **46**, 80 (1987)]
- [2] W.Wittek et al. (BEBC WA59 Coll.), *Z. Phys. C* **44**, 175 (1989)
- [3] N.M.Agababyan et al. (SKAT Coll.), IHEP Preprint-15 (2006), Serpukhov; *Yad. Fiz.* (in print)
- [4] V.V.Ammosov et al., *Fiz. Elem. Chastits At. Yadra* **23**, 648 1992 [*Sov. J. Part. Nucl.* **23**, 283 (1992)].
- [5] N.M.Agababyan et al. (SKAT Coll), YerPhI Preprint -1535 (1999), Yerevan
- [6] N.M.Agababyan et al. (SKAT Coll), *Yad. Fiz.* **66**, 1350 (2003). [*Phys. of At. Nucl.* **66**, 1310 (2003)]
- [7] N.M.Agababyan et al. (SKAT Coll), YerPhI Preprint-1578 (2002) Yerevan
- [8] N.M.Agababyan et al. (SKAT Coll), *Yad. Fiz.* **68**, 1241 (2005) [*Phys. of At. Nucl.* **68**, 1660 (2005)]
- [9] N.M.Agababyan et al. (SKAT Coll), IHEP Preprint-14 (2006), Serpukhov
- [10] D.S.Baranov et al. (SKAT Coll.), *Yad. Fiz.* **41**, 1520 (1985) [*Sov. J. Ncl. Phys.* **41**, 963 (1985)]

- [11] J.D.Jakson, Nuovo Cim. **34**, 1644 (1964)
- [12] Review of Particle Physics, J. Phys. G **33**, 38 (2006)
- [13] N.M.Agababyan et al. (SKAT Coll), IHEP Preprint-13 (2006), Serpukhov; Yad. Fiz. (in print)
- [14] A.Wroblewsry, Acta Phys. Pol. **16**, 379 (1985)
- [15] M.Adamus et al., (EHS-NA22 Coll.), Phys. Lett. B **198**, 427 (1987)
- [16] S.I.Aleshin et al., Compilation of cross sections IV, CERN-HERA, 87-01 (1987)
- [17] J.Bell et al., Phys. Rev. Lett. **40**, 1226, (1978)
- [18] H.C.Ballagh et al. (E548 Coll.), Phys. Rev. D **37**, 1744 (1988)
- [19] P.Marage et al. (WA59 Coll.), Z. Phys. C **35**, 275 (1987)
- [20] S.Willocq et al. (E632 Coll.), Phys. Rev. D **47**, 2661 (1993)

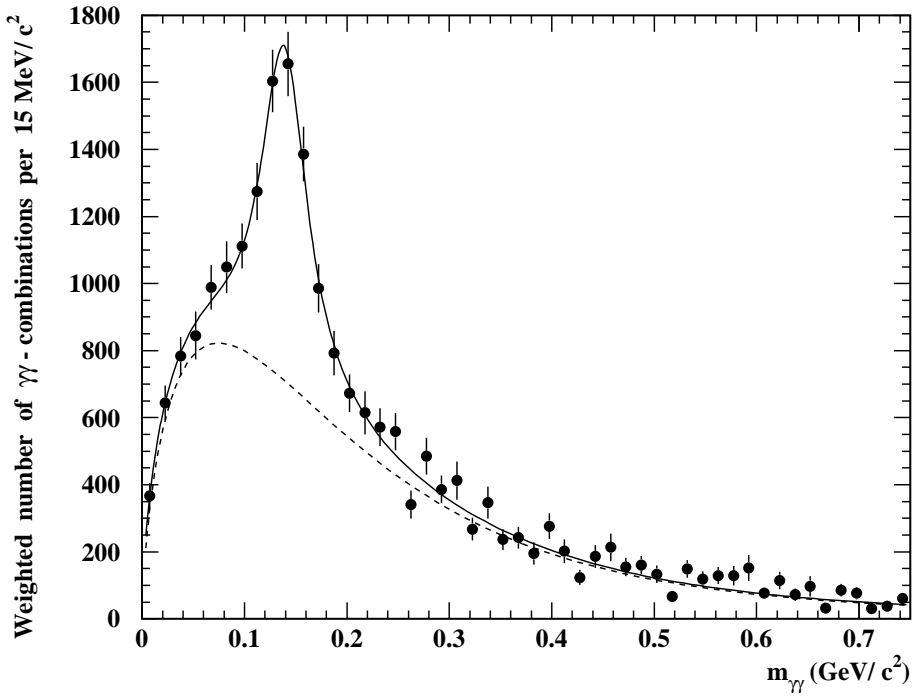


Figure 1: The two-gamma effective mass distribution. Solid curve: the fit result for the sum of Breit-Wigner and background distributions; dashed curve: the background contribution (see the text).

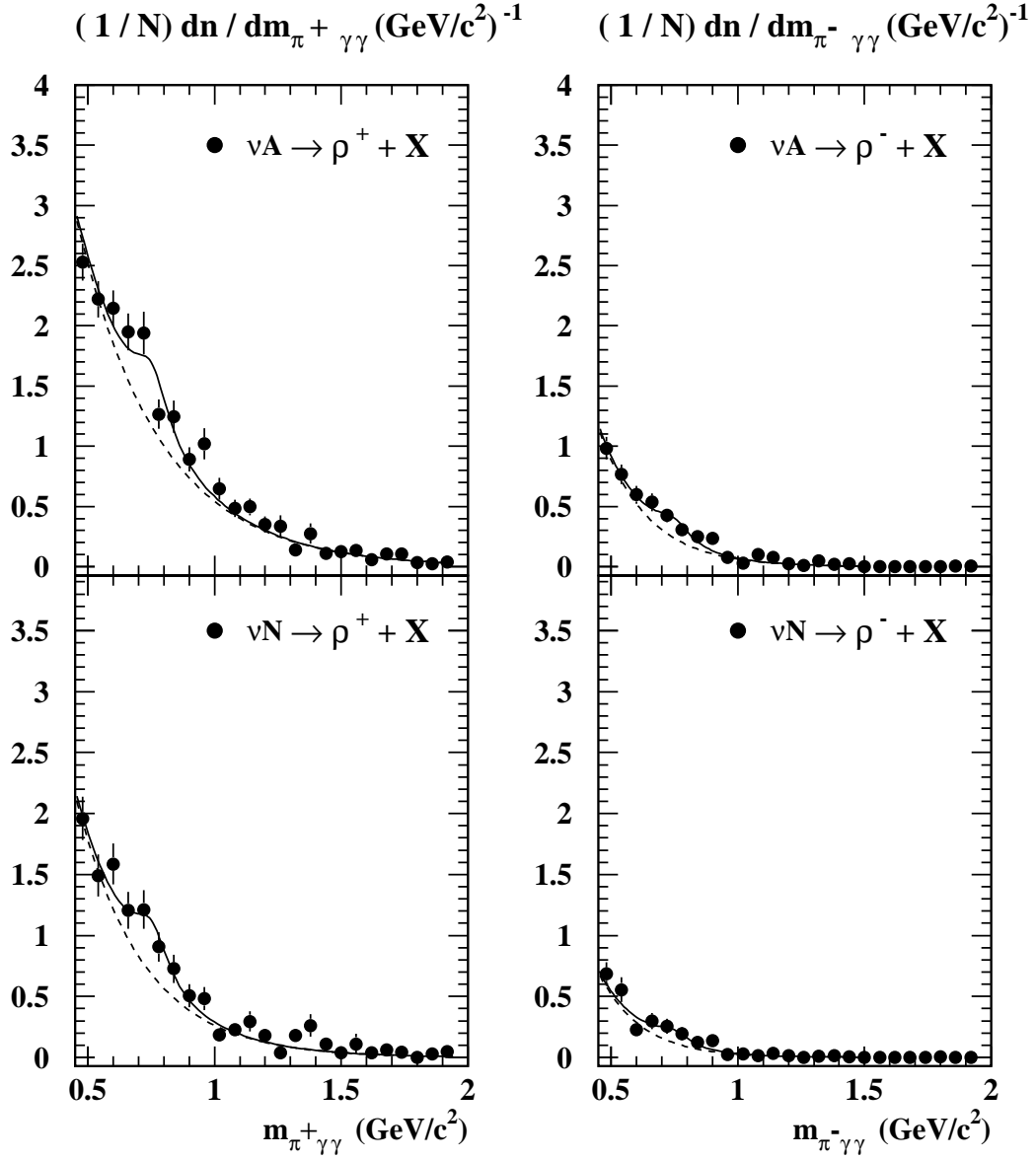


Figure 2: The effective mass distribution for systems  $(\pi^+\gamma\gamma)$  and  $(\pi^-\gamma\gamma)$  for nuclear and quasinucleon subsamples. Solid curves: the result of fit by expression (2); dashed curves: the background distribution (see the text).

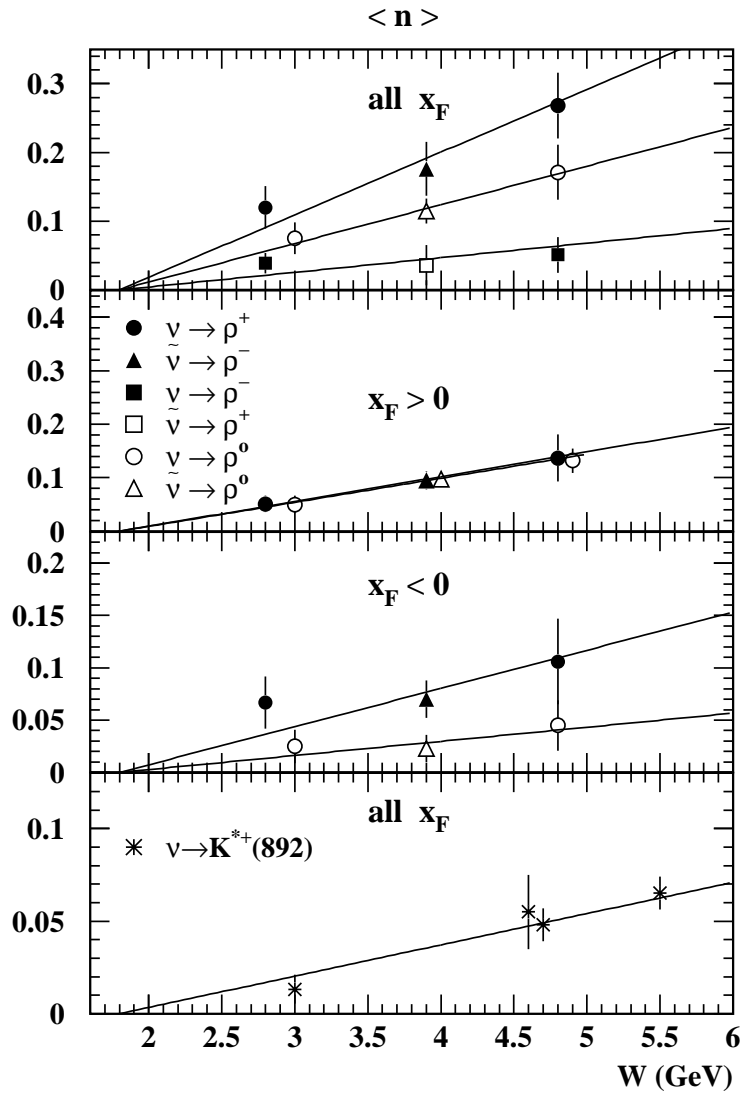


Figure 3: The  $W$  - dependence of  $\rho$  and  $K^{*+}(892)$  yields. Lines: the fit results (see the text).

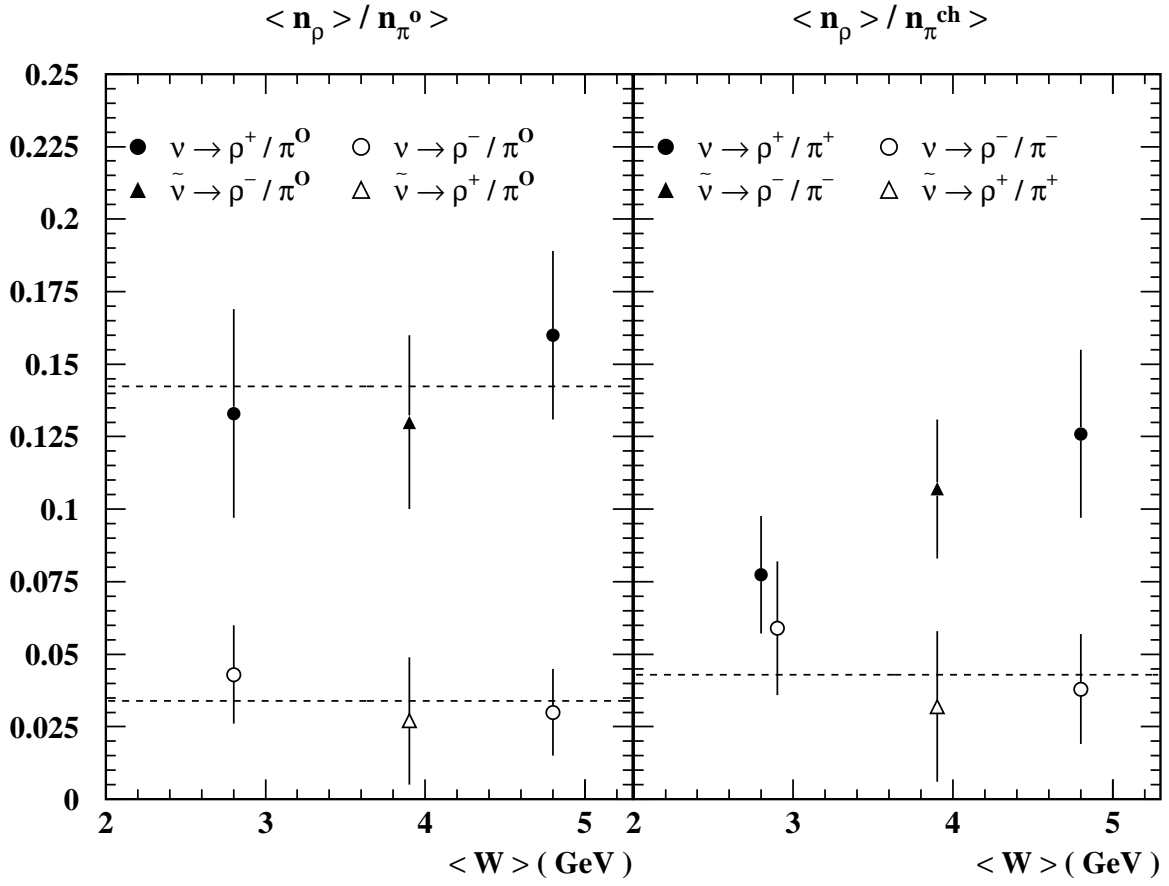


Figure 4: The  $W$  - dependence of the  $\langle n_\rho \rangle_A / \langle n_\pi \rangle_A$  ratios. Dashed horizontal lines denote the mean values (averaged over the considered  $\langle W \rangle$  - range).

Weighted number of  $\gamma\gamma$  combinations

$(1/N) dn / dm_{\pi^+\gamma\gamma} (\text{GeV}/c^2)^{-1}$

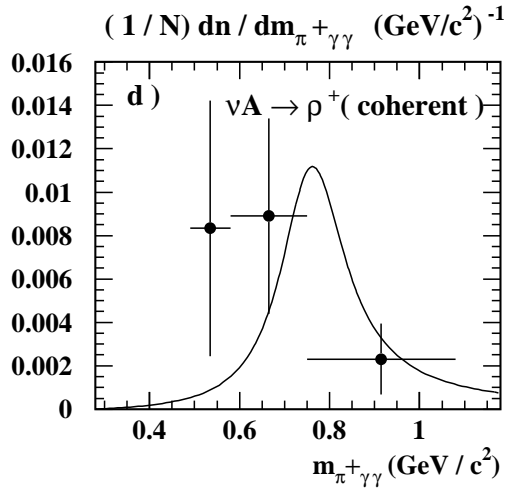
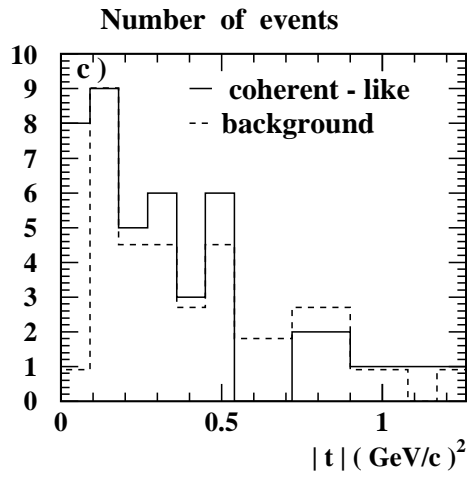
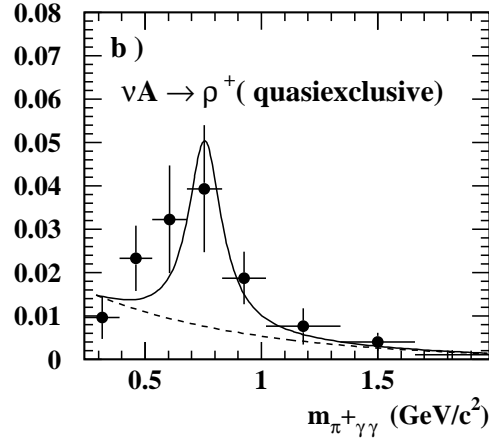
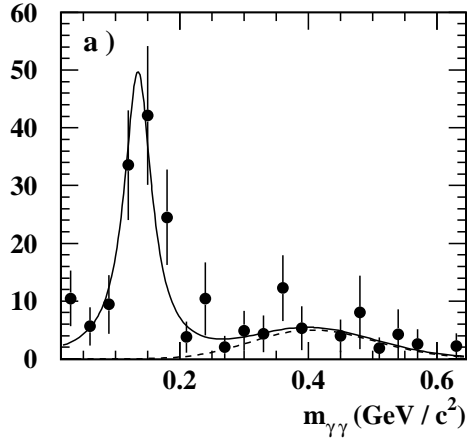


Figure 5: a) two-gamma effective mass distribution for reaction (4); the curves - as in Figure 1, but at fixed  $m_0 = 0.135 \text{ GeV}/c^2$  and  $\Gamma_0 = 0.055 \text{ GeV}$  b) the effective mass distribution for the system  $(\pi^+\gamma\gamma)$  in the reaction (4). The curves - as in Figure 2; c) the  $|t|$  - distributions for reaction (4) (solid histogram) and for background events (dashed histogram, see the text); c) the  $(\pi^+\gamma\gamma)$  effective mass distribution for coherent-like events. The curve is the fit result (see the text).

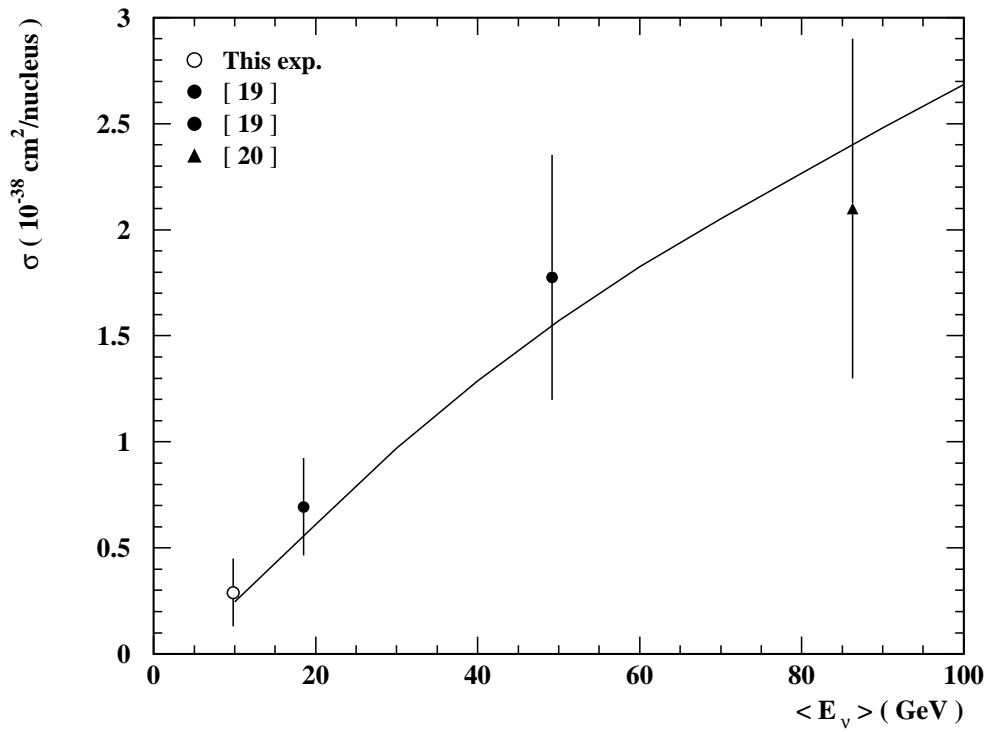


Figure 6: The  $\langle E_\nu \rangle$  - dependence of the ratio  $\sigma_\rho^{coh}$ . The curve: the theoretical prediction (taken from [19]).